CATALYTIC CRACKING OF POLYSTYRENE

Rong Lin and Robert L. White
Department of Chemistry and Biochemistry
The University of Oklahoma, Norman, OK 73019

Keywords: catalytic cracking, polymer cracking, polymer recycling

Introduction

Plastics have become the most produced materials in the United States since the mid of 1970's. The significant increase in plastics production has resulted in a similar significant increase in plastics disposal. Polystyrene is widely used in consumer product packaging and to make disposable containers. About one billion pounds of polystyrene are used in single-use disposable applications.

One approach to deal with plastic waste is to convert it into useful products, such as fuel oil and chemicals[1,2], by tertiary recycling methods. The development of effective plastic waste recycling by catalytic cracking will require detailed knowledge of the relationship between catalyst structure and cracking product distributions[3-7]. In order to compare the polymer cracking properties of different catalysts, it is preferable to examine the effects of catalysts without complications due to reactions of primary cracking products with polymer residue. Secondary reactions can be minimized by limiting the contact between primary volatile products and the catalyst/polymer mixture. This can be accomplished by maintaining high catalyst to polymer ratios and providing efficient and rapid removal of volatile products. In this paper, the importance of catalyst acidity and HZSM-5 channel structure on the volatile catalytic cracking product distributions derived from polystyrene is assessed by comparing thermal analysis results obtained from samples prepared by coating silica-alumina, HZSM-5 zeolite, and sulfated zirconia catalysts with thin layers of polystyrene.

Experimental

Samples examined in this study were: high molecular weight polystyrene (HPS), low molecular weight polystyrene (LPS), and polystyrenes coated on silica-alumina, HZSM-5, and sulfated zirconia cracking catalysts (10-20% (wt/wt)). HPS and LPS were purchased from Aldrich Chemical Company (Milwaukee, WI). The silica-alumina catalyst was provided by Condea Chemie GmbH (Hamburg, Germany). The silica-alumina catalyst contained 11.8% by weight alumina and had a surface area of 282m^2/g. The HZSM-5 zeolite catalyst was obtained from Mobil Oil (Paulsboro, NJ) and was characterized by a 355 m^2/g surface area and a 1.5% alumina content. The sulfated zirconia catalyst was synthesized following procedures described previously. The sulfated zirconia catalyst had a surface area of 157 m^2/g and contained 9% by weight sulfate. Polystyrene-catalyst samples were prepared by dissolving polystyrene in cyclohexane, adding catalyst, and then rotoevaporating the mixture to remove solvent. The resulting polymer coated catalyst samples were dried for several hours at 90°C. The apparatus used for pyrolysis-GC/MS and TG-MS measurements have been described previously. Pyrolysis separations were achieved by using a HP 5890 capillary GC with a DB-5 column (0.25 μm film thickness). The gas chromatograph oven temperature program consisted of a 2 min isothermal period at -50 °C followed by a 10 °C/min ramp to 280 °C, and then another isothermal period at 280 °C for 5 minutes. For TG-MS studies, samples were heated from 50 °C to 600 °C in He at rates of 1, 10, 25, and 50 °C/min. For TG-GC/MS studies, a Valco Instruments, Inc. (Houston, TX) heated eight external volume sample injector was employed to divert small volumes (ca. 20 μL) of TG effluent into a 30 m DB-5 capillary column (0.25 μm film thickness) for GC/MS analysis. A 5 °C/min heating rate from 50 °C to 600 °C in 20 mL/min He was used to heat samples in the thermogravimetric analyzer. When samples reached 100 °C, TG effluent was sampled. Above 100 °C, TG effluent sampling was repeated at 3 min intervals during TG-GC/MS analysis. A 5 mL/min He carrier gas flow rate through the TG-GC/MS chromatographic column was employed and the column temperature was maintained at 100 °C during separations. TG-GC/MS column effluent was split prior to entering the mass spectrometer to maintain an ion source pressure of 5 x 10^{-5} torr.

Results and Discussion

Pyrolysis-GC/MS results obtained for polymers and polymer-catalyst samples pyrolyzed at 400°C were compared to investigate the effects of different catalysts and initial polymer molecular weight on cracking product distributions. Tables 1 and 2 contain the volatile product distributions derived from chromatograms for neat polymers and polymer-catalyst samples. Thermal degradation of neat polystyrene samples produced primarily styrene monomer along with substantial amounts of dimer and trimer. By examining the volatile product distributions for high molecular weight polystyrene (HPS) and low molecular weight polystyrene (LPS), it was found that the relative yield of trimer was about three times that of the dimer and the relative yield of styrene was greater for the HPS sample than for the LPS sample. However, in the presence of catalysts, the most abundant volatile product was benzene, and very little styrene was detected. Benzene comprised about 30% of the volatile material produced from the polymer-Si/Al and polymer-ZrO_2/SO_4 samples, and over 50% from the polymer-HZSM-5 zeolite samples. Other volatile products detected from the polymer-catalyst samples with relative yields over 1% included: alkyl benzenes, indanes, indenes, and naphthalenes. For both LPS and HPS samples, the relative yields of alkyl benzenes were greatest for samples containing Si/Al and ZrO_2/SO_4 catalysts, whereas polymer-HZSM-5 samples produced fewer alkyl benzenes but significantly larger quantities of indenes.

TG-MS was employed to correlate the evolution of volatile thermal decomposition products with sample weight loss and to calculate volatilization activation energies. Weight loss curves obtained by heating samples at 10 °C/min in He are shown in Figures 1 and 2. Compared to neat polymer thermal decompositions, all three catalysts lowered the temperature at which significant sample weight loss occurred. The catalytic effect was greatest for the samples containing the ZrO_2/SO_4 catalyst. By examining the weight loss curves, it was found that, for the same catalysts, the weight loss onset temperature was lower for the LPS polymer than for the HPS polymer. The polymer-ZrO_2/SO_4 samples exhibited two distinct steps in their weight loss curves. TG effluent mass spectra indicated that the low temperature weight loss step was caused by polystyrene decomposition. The high temperature step resulted from catalyst decomposition and corresponded to SO_2 evolution.

Neat polymer and polymer-catalyst samples were subjected to TG-MS analysis in He with heating rates of 1, 10, 25, and 50 °C/min to investigate the effects of catalysts on volatilization activation energies calculated by using the Friedman method. The activation energy for the neat HPS polymer was slightly higher than that for the neat LPS polymer. For samples containing the same catalyst, those containing the LPS polymer exhibited a lower volatilization activation energy than those containing the HPS polymer. The lowest volatilization activation energies were calculated for samples containing ZrO_2/SO_4 catalyst.

Mass spectra obtained during TG-MS analyses could not be used to profile the temperature dependent evolutions of the primary thermal decomposition products because species specific ions could not be identified. By placing a gas chromatograph between the thermogravimetric analyzer and mass spectrometer, it was possible to separate the primary volatile products generated in the thermogravimetric analyzer prior to mass analysis. Figures 3 and 4 contain plots of TG-GC/MS chromatographic peak areas (integrated total ion current) as a function of sample temperature for selected products. For all samples analyzed, benzene was by far the most abundant volatile product. All of the polymer-catalyst samples produced alkyl benzenes and indanes, however samples containing HZSM-5 catalyst produced significantly less than the other samples. Styrene and indenes were only detected from samples containing HZSM-5 catalyst.

Formation of the primary polystyrene catalytic cracking volatile products can be explained by consequences of initial electrophilic attack on polymer aromatic rings by protons. Most of the products detected by pyrolysis-GC/MS and TG-GC/MS can be derived from ortho ring protonation. The initial step in polystyrene cracking is protonation of polymer aromatic rings. Ortho protonation can easily lead to benzene evolution and the formation of a secondary macro cation, or may result in chain shortening, yielding a chain end cation and a saturated chain end.

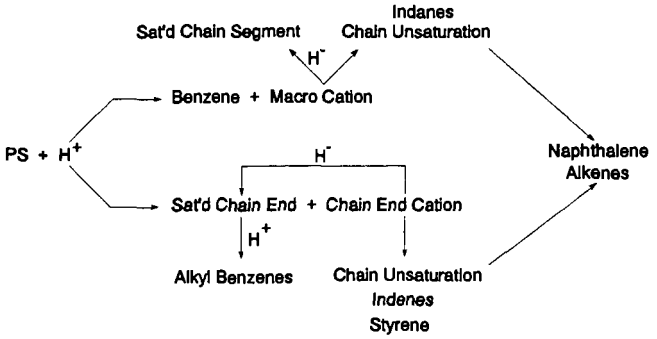

After protonation of chain end aromatic rings, β-scission can yield alkyl benzenes. Beta-scission and rearrangement of chain end cations can lead to chain unsaturation or the formation of styrene and indenes. Cyclization of the secondary macro cations can lead to the formation of indanes, or after rearrangements and β-scission of macro cations, chain unsaturation can be formed. Also, macro cations can undergo hydride abstraction leading to the formation of saturated chain segments. A consequence of chain unsaturation might be the formation of conjugated polyene segments that may subsequently cyclize to form naphthalenes.

Conclusions

Effects of different catalysts and initial molecular weights of polystyrene on catalytic cracking product distributions were studied. Benzene was produced by polystyrene catalytic cracking at temperatures as low as 130 °C for LPS-ZrO_2/SO_4 samples. This suggests that low temperature benzene evolution may result primarily from chain ends, which would be more abundant for the LPS polymer than for the HPS polymer. Chain end aromatic rings should be somewhat more susceptible to electrophilic attack because electron release from the polymer backbone into these rings should be slightly greater than for other aromatic rings in the polymer. Because the samples containing the LPS polymer had more chain ends than the HPS polymer, low temperature reaction rates for the LPS polymer would be consistently higher than for the HPS polymer, which would lead to the observed higher benzene evolution rates at low temperature for samples containing the LPS polymer. Benzene can be easily formed after aromatic ring protonation, but that formation of other volatile products is more difficult and may require additional reactions, such as macro cation rearrangement, hydride abstraction, or successive protonations.

Acknowledgment

Financial support for this work from the National Science Foundation (CTS-9509240) is gratefully acknowledged.

References

1. D.S. Scott, S.R. Czernik, J. Piskorz, D.Radlein, *Energy & Fuels*, 4, 407(1990).
2. Y. Ishihara, H. Nambu, T. Ikemura, T. Takesue, *J. Appl. Polym. Sci.*, 38, 1491(1989).
3. M. Yamamoto, I. Suzuko, S. Yamanaka, *Nippon Kagaku Kaishi*, 5, 802(1976).
4. T. Ogawa, T. Kuroki, S. Ide, T. Ikemura, *J. Appl. Polym. Sci.*, 27, 857(1981).
5. Cr.I. Simionescu, C. Vasile, P. Onu, M. Sabliovschi, G. Moroi, V. Barboiu, D. Ganju, M. Florea, *Thermochim Acta*, 134, 301(1988).
6. Z. Zhang, T. Hirose, S. Nishio, Y. Morioka, N. Azuma, A. Ueno, H. Ohkita, M. Okada, *Ind. Eng. Chem. Res.*, 34, 4514(1995).
7. G. Audisio, F. Bertini, P.L. Beltrame, P. Carniti, *Polym. Degrad. Stab.*, 29, 191(1990).

Table 1. LPS Decomposition Products at 400°C

Product	Neat LPS	LPS-Si/Al	LPS-ZrO_2/SO_4	LPS-HZSM-5
benzene		31	31	52
toluene	1	1	3	3
ethyl benzene		20	10	5
styrene	41	1		1
isopropyl benzene		6	6	
methyl styrene				
indane		10	10	7
indene		1		3
methyl indane		17	25	7
methyl indene				3
naphthalene		4	2	7
2-methyl naphthalene		4	2	6
1-methyl naphthalene		2	2	
dimer	11			
trimer	35			

Table 2. HPS Decomposition Products at 400°C

Product	Neat HPS	HPS-Si/Al	HPS-ZrO_2/SO_4	HPS-HZSM-5
benzene		30	33	60
toluene			3	2
ethyl benzene		14	12	2
styrene	68	4		2
isopropyl benzene		9	8	
methyl styrene				1
indane		15	9	3
indene		1		3
methyl indane		17	8	6
methyl indene				3
naphthalene		3	7	3
2-methyl naphthalene		2	5	3
1-methyl naphthalene		2	5	1
dimer	6			
trimer	16			

Table 3. Volatilization Activation Energies (kcal/mol)

Catalyst	LPS	HPS
none	46.4 ± 1.2	48.5 ± 0.8
Si-Al	33.8 ± 0.5	38.6 ± 0.5
ZrO_2/SO_4	24.4 ± 2.9	28.9 ± 1.9
HZSM-5	34.6 ± 0.5	36.0 ± 1.3

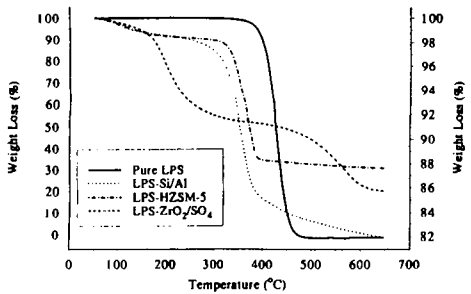

Figure 1. TG weight loss curves for neat LPS (left axis) and LPS-catalyst samples (right axis) obtained by heating samples at a rate of 10 °C/min.

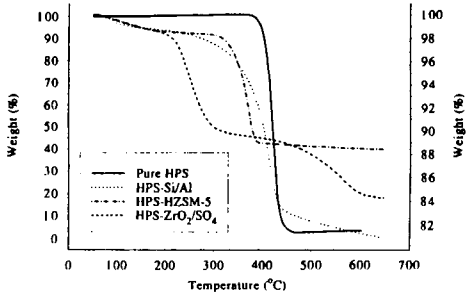

Figure 2. TG weight loss curves for neat HPS (left axis) and HPS-catalyst samples (right axis) obtained by heating samples at a rate of 10 °C/min.

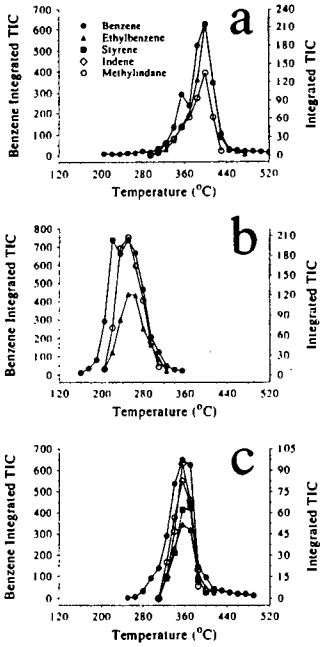

Figure 3. TG-GC/MS chromatographic peak areas derived from (a) LPS-Si/Al, (b) LPS-ZrO_2/SO_4; and (c) LPS-HZSM-5.

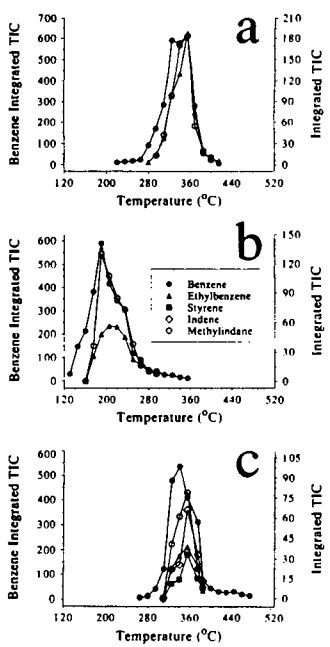

Figure 4. TG-GC/MS chromatographic peak areas derived from (a) HPS-Si/Al, (b) HPS-ZrO_2/SO_4; and (c) HPS-HZSM-5.